Mechanics of rough contacts in elastic and viscoelastic thin layers

Mechanics of Rough Contacts in Elastic and Viscoelastic Thin Layers

C. Putignano[a,*], G. Carbone[b], D. Dini[a]

[a] *Department of Mechanical Engineering, Imperial College London, Exhibition Road, South Kensington, London,SW7 2AZ, United Kingdom.*
[b] *TriboLAB-Dipartimento di Ingegneria Meccanica e Gestionale, Politecnico di Bari, V.le Japigia 182, 70126 Bari-ITALY.*

Abstract

Contact mechanics between rough solids usually relies on the half-space approximation, which assumes that the contact area dimension is much smaller than the thickness of the layers of materials that characterise the surfaces of the contacting bodies. However, such simplifying assumption is often inadequate when industrially relevant applications are considered, in particular those of biomechanical interest. Indeed, a large variety of systems, including not only classical engineering applications such as gear boxes, shafts, tyres, etc., but also biological tissues such as human skin, is characterised by superficial coatings; very often the mechanical properties of these coatings are very different from those of the bulk region of the bodies in contact. The aim of this paper is to shed light on the role played by the thickness of the layer of material used as a coating, with specific focus on the contact between a rigid rough surface and a thin deformable layer bonded to a rigid substrate.

*Corresponding author. Phone: +44 020 7594 7064
Email address: c.putignano12@imperial.ac.uk (C. Putignano)

Starting from a recently developed Boundary Element formulation (Carbone and Putignano, 2013), we derive a methodology which accounts for finite thickness by a corrective coefficient modulating the classical Greens function, and extends our analyses to periodic domains. This enables to avoid border effects and provides an innovative tool to tackle viscoelastic contacts with realistic roughness. This is exploited to perform a thorough investigation of the mechanisms responsible for frictional losses in layered systems characterised by different materials, thickness and loading conditions. Results show that decreasing the layer thickness corresponds to an increase in the contact stiffness. Furthermore, in the case of viscoelastic layer, particular attention has to be paid to the changes in the viscoelastic dissipation due to the finite thickness of the surface layer.

Keywords: viscoelastic contact mechanics, finite thickness, boundary element methods.

1. Introduction

In the last two decades, contact mechanics between rough surfaces has assumed a prominent role in engineering research, with hundreds of papers employing analytical, numeric and experimental approaches to shed light on several issues of the problem. Beyond pure theoretical interest, such vast research effort is directly linked to the wide variety of technologically important phenomena strongly influenced by roughness of the surfaces in contact problems. Indeed, in any real tribo-system, multiscale roughness, complex

rheological behavior of contacting solids, and the presence of multi-phase components combine to determine important macroscopic properties such as friction, dissipation, wear, contact stiffness. This has a tremendous impact on a large number of engineering applications. On one side, we have quite traditional components requiring to be redesigned according to the trend of modern engineering that prompts to boost reliability and energy efficiency: car tyres and mechanical rubber seals are possible examples where a better understanding of the energy dissipation and, in the second case, of the percolation mechanism can really improve a everyday-life component. On the other side, there is a wide variety of innovative pioneering devices that, to be fully developed, need a sharp improvement in our theoretical knowledge: novel bio-inspired adhesives ([1], [10], [18], [19], [20], [27],[23],[28]) and mechanical and electrical micro systems (MEMS) ([2], [1]) have, for example, a limited diffusion owing to the significant limitations in the understanding of their physical working principles.

In order to deal with these challenging issues, a variety of methodologies have been proposed in the scientific literature. Historically, the problem has been firstly approached by developing the so-called multi-asperity models aimed to solve the contact between elastic rough surfaces ([41],[42],[43],[44],[45]) : basically, these methodologies consider the rough surfaces constituted by asperities -with a certain distribution of radii of curvature and height distribution- which behave like independent Hertzian punches. This class of theories, which does not take into account the mutual interaction between

asperities in contact, has a further drawback: they reduce the shape of contact spots to Hertzian circular or elliptical contacts and, thus, neglect the fact that contact regions present fractal-like boundaries (see [13]) and can assume non-simply connected shapes. This entails a variety of problems in the correct estimation of many prominent quantities, including the contact area and the contact stiffness. In particular, multi-asperity contact models have been shown in [32] to predict linearity between applied load and true contact area only for extremely small applied loads. This is in contrast with experimental and numerical evidences and, more importantly, seems not to be coherent with the Amontons–Coulomb's friction law, asserting the direct proportionality between the friction force and the load and, therefore, suggesting the direct proportionality between the real contact area and the applied load. Corrections to include interactions have also been proposed ([53].); however, they only partially solve the issues identified above. In the last decade, Persson has attempted to overcome these problems by proposing a different approach ([12], [14]) based on the assumption that the contact pressure probability distribution is governed by a diffusive process as the magnification at which we observe the interface is increased. The theory is formulated in such a way that in full-contact conditions its results are exact, while in the case of partial contacts, although it provides only an approximate solution, is at least qualitatively valid as it still predicts linearity between contact area and load (see e.g. Ref. [34] and [35] for a more detailed discussion of the problem). Interestingly, Persson has developed his theory

to account for materials with a linear viscoelastic rheology, thus providing predictions for the viscoelastic friction ([12], [14]) . Furthermore, although in this case the theory provides good qualitative trends and helps understanding the behavior of contacts in the presence of complex rheology, its quantitative validity is still widely debated; this can have dramatic implications for many practical applications.

Given all these issues affecting analytical theories, a lot of different numerical approach have been developed to get quantitatively and qualitatively accurate results. The variety of the proposed techniques includes finite element methods (FEM) ([56]), boundary elements methods (BEM) ([54], [33],[27],[47]), molecular dynamics simulations ([62], [61], [63]) and hybrid approaches ([64], [65]). In all these cases, getting the full numerical convergence is a crucial point that deeply influences the reliability of the results (see [48] for a detailed discussion). The actual relation between real contact area and load has been, for example, widely debated since, as shown in [48], it strongly depends on the capability of converging. All these issues are mainly due to the large number of length scales (covering several order of magnitudes) involved in the rough contact. This point becomes even more important when viscoelasticity is considered. In this case, the material time-dependent behavior , in general, require to consider also the time domain and this really increases the simulation computational cost. Recently, thanks to new computational techniques and more powerful computational resources getting widely available, significant steps forward have been done

both for elastic and viscoelastic contacts ([34], [63], [55],[31]), but a lot of work remains to be done.

In this paper, in particular, we focus on an issue that has not received so far the right consideration it would have deserved: this is the study of the effects related to the finite thickness of the bodies in contact. Indeed, the almost totality of the boundary element methodologies formulated in the real space and presented in literature ([54], [33],[27],[47]) relies on the half-space assumption, which consists in assuming that the thickness of the solids in contact is much larger than the contact area. In principle, boundary elements techniques derived in the Fourier space can tackle contact problems with surfaces characterised by layers of finite thickness ([68],[66],[67]); however, systematic investigations of the effects related to the thin layer mechanics are not common in literature. Furthermore, studies performed adopting finite element methodologies ([56],[24], [25]), molecular dynamics simulations ([62], [61], [63]) and hybrid techniques ([64], [65]), which intrinsically consider the bulk of the contact solids in their formulation, usually do not pay attention to the finite size effects and employs models with thickness values that are believed, on heuristic basis, to be large enough to avoid any influence given by the thickness. However, as widely shown for smooth contact mechanics problems ([57],[58]), finite thickness has often to be accounted for: many systems -for example, all components with coatings- have a surface layer whose characteristics are very different from the remaining bulk region of contact body. In all these cases, the half-space assumption can lead

to large errors in the estimations not only of contact stresses and strains, but also friction and wear. This is relevant not only for many industrial components, including turbomachinery blades, gears, seals, but also biological tissues. Human skin is just an example of a layered system where finite size effects cannot be neglected ([59], [60]). To tackle contact problems related to these interesting topics, we derive a boundary element formulation which modifies the methodologies presented in [33] and [52] to account for the finite thickness layers made of both elastic and viscoelastic materials. The formulation is further improved to include a fast numerical periodic solver that allows simulating large contact domains (Section II). The proposed methodology is then used to explore the behavior contacts between a rough rigid surface and an elastic or viscoelastic layer of finite thickness bonded to a rigid substrate. Results are presented and discussed in Section III, when the proposed methodology is also used to unravel some of the subtleties linked to the specific behavior of viscoelastic layers.

2. Formulation

The modelling technique employed in this paper is a boundary element method (BEM); such methodology is extensively used for contact mechanics problems ([54], [33],[27]), and relates surface displacement to interfacial pressure by means of a convolution integral. In particular, Ref. [33] observed that, for rough periodic contacts, the displacement is the sum of two terms: the first is equal to the mean displacement $\mathbf{u}_{\mathrm{m}}$; the second $\mathbf{v}\left(\mathbf{x},z\right) =$

$\mathbf{u}\left(\mathbf{x},z\right)-\mathbf{u}_{\mathrm{m}}\left(z\right)$, where $\mathbf{x}$ is the in-plane position vector, is just the additional displacement related to the asperities-induced deformation. In a periodic domain made of square cells, $D=[(-\lambda/2,\lambda/2)\times(-\lambda/2,\lambda/2)]$, where λ is the cell size, and subjected to periodic load conditions, it can be shown that the mean displacement $u_{\mathrm{m}}=\mathbf{u}_{\mathrm{m}}\left(z=0\right)$ of the elastic body at the interface and, therefore, the total layer surface displacement $u_z\left(\mathbf{x},z=0\right)=u_z\left(\mathbf{x}\right)$ are unbounded; therefore, only the term $v\left(\mathbf{x},z=0\right)=v\left(\mathbf{x}\right)=u_z\left(\mathbf{x}\right)-u_{\mathrm{m}}$ is finite. As a matter of fact, for this kind of systems, the problem is formulated in such a way that the displacements $v\left(\mathbf{x}\right)$ are related to the interfacial stresses $\sigma(\mathbf{s})$ by:

$$v(\mathbf{x})=\frac{1}{E}\int_D d^2s\mathcal{L}(\mathbf{x}-\mathbf{s})\sigma(\mathbf{s}),\qquad \mathbf{x}\in D \tag{1}$$

with $\mathcal{L}\left(\mathbf{x}\right)$ being the periodic Green's function defined as

$$\mathcal{L}\left(\mathbf{x}\right)=\sum_{k=-\infty}^{+\infty}\sum_{h=-\infty}^{+\infty}G\left(\mathbf{x}-\mathbf{x}_{hk}\right)-G_m \tag{2}$$

where E is the elastic modulus of the materia, and $\mathbf{x}_{hk}=\left(x+\lambda h\ ,\ y+\lambda k\right)$. In such a relation

$$G\left(\mathbf{x}\right)=-\frac{(1-\nu^2)}{\pi\left|\mathbf{x}\right|} \tag{3}$$

is related to the Boussinesq solution for the elastic half-space [38], and G_m is equal to $G_m=\lambda^{-2}\sum_{k=-\infty}^{+\infty}\sum_{h=-\infty}^{+\infty}\int_D G\left(\mathbf{x}-\mathbf{x}_{hk}\right)d^2x$. In Ref. [33], $\mathcal{L}\left(\mathbf{x}\right)$ is shown to be equal to elastic displacement at the interface $u_z(x)$ caused by a periodically applied self-balanced normal stress distribution.

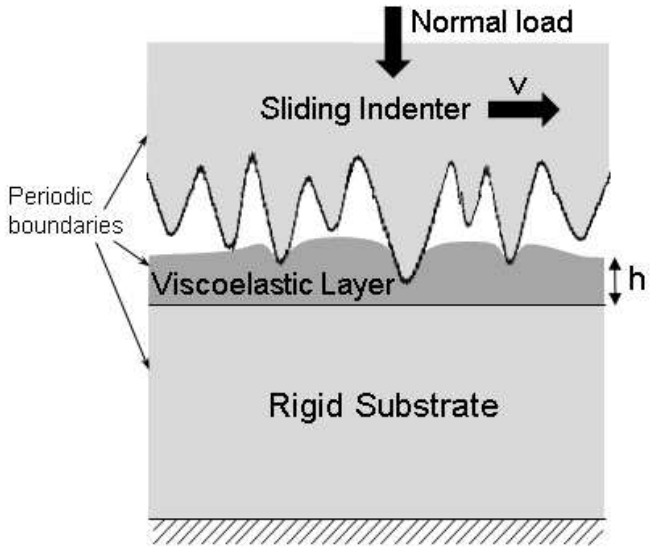

Figure 1: A rough rigid surface sliding on a viscoelastic layer attached to a rigid substrate.

Such a formulation has to be modified to account for the finite thickness of the contact layer. Starting from the formulation proposed in Ref. [10], we re-write Eq. (1) in the following way:

$$v(\mathbf{x})=\frac{1}{E}\int_D d^2s\mathcal{T}(\mathbf{x}-\mathbf{s})\sigma(\mathbf{s}), \quad \mathbf{x}\in D \tag{4}$$

with the new periodic Green's function $\mathcal{T}(\mathbf{x})$ accounting for the finite thickness and being equal to:

$$\mathcal{T}(\mathbf{x}) = \sum_{k=-\infty}^{+\infty}\sum_{h=-\infty}^{+\infty}\Theta\left(\frac{|\mathbf{x}-\mathbf{x}_{hk}|}{h}\right)G(\mathbf{x}-\mathbf{x}_{hk})-\mathcal{T}_{\mathrm{m}} \tag{5}$$

The mean term $\mathcal{T}_m$ is, now, equal to

$\mathcal{T}_{\mathrm{m}} = \lambda^{-2} \sum_{k=-\infty}^{+\infty} \sum_{h=-\infty}^{+\infty} \int_D \Theta\left(|\mathbf{x} - \mathbf{x}_{hk}| / h\right) G\left(\mathbf{x} - \mathbf{x}_{hk}\right) d^2x$ and $\Theta\left(|\mathbf{x}| / h\right)$ is the corrective parameter introduced to account for the slab thickness h:

$$\Theta\left(r/h\right) = \int_0^{+\infty} dw S\left(wh/r\right) J_0\left(w\right), \tag{6}$$

with $S\left(wh/r\right)$ being a correction term which accounts for different constraints or boundary conditions [10]. $J_0\left(w\right)$ is the zero-th order Bessel function. In the case we are interested in this paper, which refers to a deformable slab of thickness h sandwiched between a flat rigid plate and a rigid substrate (see Fig. 1), $S\left(wh/r\right)$ assume the following expression [10]:

$$\mathcal{S}\left(wh/r\right) = \frac{\left(3-4\nu\right)\sinh\left(2wh/r\right) - 2wh/r}{5 + 2\left(wh/r\right)^2 - 4\nu\left(3-2\nu\right) + \left(3-4\nu\right)\cosh\left(2wh/r\right)} \tag{7}$$

Figure 2a shows how $\Theta\left(r/h\right)$ approaches the unit value at relatively low values of r/h, i.e. in half-space conditions, and rapidly vanishes as $r/h \to \infty$. The dimensionless Green's function, $\mathcal{T}\left(\mathbf{x}\right)/\lambda$, is, then, plotted in Figure 2b for a composite Young modulus $E^* = E/(1-\nu^2) = 1$ Pa , a Poisson ratio $\nu = 0.5$ and several values of the thickness t/λ. We may observe, *inter alia*, that, since the volume has to be preserved, $\mathcal{T}\left(\mathbf{x}\right)$ can invert its sign in some regions.

Furthermore, the corrective coefficient, while modulating the fondamental function $G\left(\mathbf{x}\right)$, also has a strong effect on the correlation length $l_c(h)$, here defined as the length at which $G\left(\mathbf{x}\right)$ vanishes. l_c is infinite in the case of a half-space, but is finite for finite values of the thickness h and tends

[a]

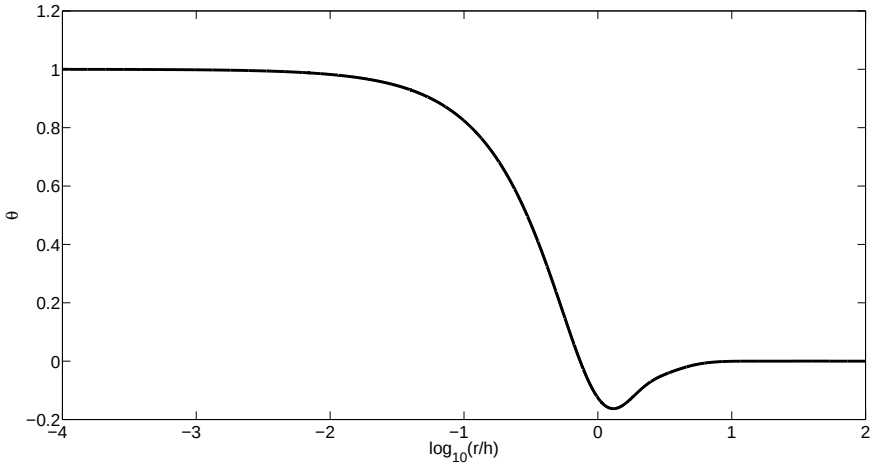

[b]

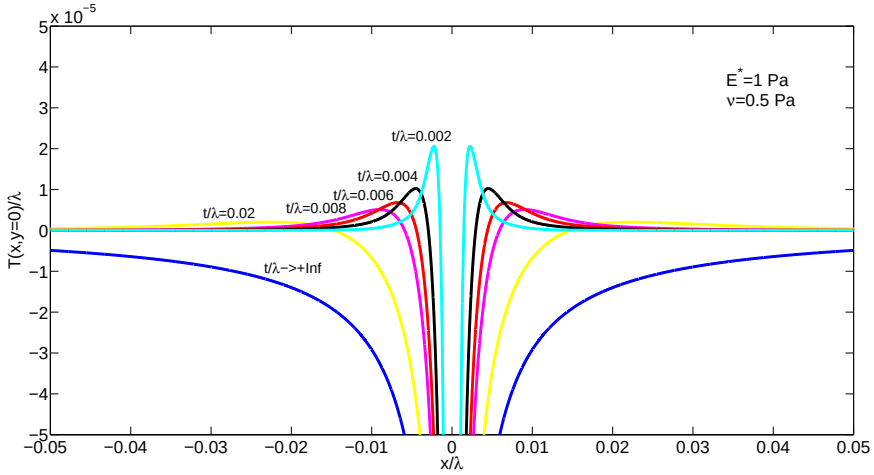

Figure 2: (a) The correction factor $\Theta\left(r/h\right)$ and (b) the Green's fiunction $T(x,y=0)/\lambda$ as a function of the ratio r/h in a log-linear diagram.and the dimensionless abiscissa x/λ .

to vanish when $h \to 0$. Indeed, by looking at Figure 2, we observe that $\Theta(r/h)$ vanishes when $r/h \approx 10$ and, consequently, l_c is equal to $l_c \approx 10h$. In other words, finite thickness introduces, in addition to the specific modulation related to the form of $\Theta(r/h)$, a cut-off of the contact problem response function. This means that a variation in h directly affects the contact stiffness. In particular, when h vanishes and, therefore, the deformable layer disappears, the contact becomes infinitely stiff as the surface and the substrate, being both rigid, get in contact.

Furthermore, we observe that, given the particular form of the problem under investigation, when we solve Eq. (4) following the iterative procedure described in [33, 34, 48], the discretization step must be carefully selected: this must be much smaller than the correlation length for the specific layer thickness under investigation.

Turning now to more complex material rheology, in Ref. [34], an innovative formulation has been presented to deal with the sliding contact between linearly viscoelastic bodies, i.e. materials whose viscoelastic modulus $E(\omega)$ is equal to $1/E(\omega) = 1/E_\infty + \int_0^\infty d\tau \mathcal{C}(\tau) / (1 + i\omega\tau)$ ([26]), with E_∞ being the elastic glass modulus, $\mathcal{C}(\tau)$ a strictly positive function usually defined as the creep spectrum, and τ the relaxation time [26] [50]. A viscoelastic Green's function $G_V(\mathbf{x}, \mathbf{v})$ has been introduced and the problem has been solved by means of the same techniques available for elastic contacts ([3]). In particular, in Ref. [3] it is shown that the viscoelastic Green's function $G_V(\mathbf{x}, \mathbf{v})$ can be calculated using Eq. (3) as

$$G_V(\mathbf{x},\mathbf{v}) = J(0)G(\mathbf{x}) + \int_0^{+\infty} dt G(\mathbf{x}+\mathbf{v}t)\dot{J}(t), \tag{8}$$

with $J(t)$ being the linear viscoelastic creep function [the symbol $(\cdot)$ stands for the time derivative].

Such a methodology has already been successfully employed in Ref. [52] to shed light on some of the fundamental issues marking the viscoelastic contact mechanics between rough solids. Here the authors extend this formulation not only to account for the role played by the finite thickness layer but also to consider a fully periodic domain. Indeed, the original formulation proposed in Ref. [34] is non-periodic; therefore, such an approach could be affected by the ill-posedness of the boundary conditions when it is employed to study quite large contact areas and the effect of the presence of layered bodies. Periodicity has to be therefore implemented. To do this, we could follow the same path proposed for elastic materials by employing Eq. 2 to define the viscoelastic periodic function $\mathcal{G}(\mathbf{x},\mathbf{v})$:

$$\mathcal{G}(\mathbf{x},\mathbf{v}) = G_P(\mathbf{x},\mathbf{v}) - \mathcal{G}_m(\mathbf{v}) \tag{9}$$

where

$$G_P(\mathbf{x},\mathbf{v}) = \sum_{k=-\infty}^{+\infty}\sum_{h=-\infty}^{+\infty} G_V(\mathbf{x}-\mathbf{x}_{hk},\mathbf{v}) = \sum_{k=-\infty}^{+\infty}\sum_{h=-\infty}^{+\infty}\left\{\frac{1}{E_\infty}G(\mathbf{x}-\mathbf{x}_{hk})\,\Theta\left(\frac{|\mathbf{x}-\mathbf{x}_{hk}|}{h}\right)\right.$$
$$\left. + \int_0^{+\infty} d\tau\mathcal{C}(\tau)\int_0^{+\infty} dz G(\mathbf{x}-\mathbf{x}_{hk}+\mathbf{v}\tau z)\,\Theta\left(\frac{|\mathbf{x}-\mathbf{x}_{hk}+\mathbf{v}\tau z|}{h}\right)\exp(-z)\right\}$$

$$\mathcal{G}_m(\mathbf{v}) = \lambda^{-2} \sum_{k=-\infty}^{+\infty} \sum_{h=-\infty}^{+\infty} \int_D d^2x G_V(\mathbf{x} - \mathbf{x}_{hk}, \mathbf{v}) \tag{10}$$

As in the elastic case, the periodic Green's function $\mathcal{G}(\mathbf{x}, \mathbf{v})$ is equal to the displacement at the interface caused by a periodically applied self-balanced normal stress distribution. We observe that calculating $\mathcal{G}(\mathbf{x}, \mathbf{v})$ in this way, with no further development, would be numerically inefficient as an integral term should be evaluated for each point of the double series and for each creep coefficient. Computational cost can be largely decreased by manipulating Eqs. 9-10: rather than periodizing directly the viscoelastic Green's function as just shown, we employ the periodic function $\mathcal{T}(\mathbf{x})$ to re-define the viscoelastic Green's function. In other words, we exploit the elastic-viscoelastic Green's function relation, stated in Eq. 8, but use, in this case, $\mathcal{T}(\mathbf{x})$ instead of $G(\mathbf{x})$, i.e.

$$G_P(\mathbf{x}, \mathbf{v}) = \frac{1}{E_\infty} \mathcal{T}(\mathbf{x}) + \int_0^{+\infty} d\tau \mathcal{C}(\tau) \int_{0^+}^{+\infty} dz \exp(-z) \mathcal{T}(\mathbf{x} + \mathbf{v}\tau z) \tag{11}$$

This enables us to formulate the periodic viscoelastic rough contact problem in the following form

$$\begin{aligned} v(\mathbf{x}) &= \frac{1}{E_\infty} \int_D d^2s \mathcal{T}(\mathbf{x} - \mathbf{s}) \sigma(\mathbf{s}) \\ &\quad + \int_D d^2s \int_0^{+\infty} d\tau C(\tau) \int_{0^+}^{+\infty} dz \exp(-z) \mathcal{T}(\mathbf{x} + \mathbf{v}\tau z - \mathbf{s}) \sigma(\mathbf{s}) \end{aligned} \tag{12}$$

By introducing the periodic function $\mathcal{T}(\mathbf{x})$ in the formulation of the viscoelastic Green's function rather than directly periodizing the viscoelastic Green's function, as shown in [33] for the elastic case, we introduce very large computational savings, with two or three order of magnitudes increase in processing speed, therefore enabling solving problems whose size would be inaccessible to alternative solvers, at least, in the real space. In this way, we are able to account for both periodicity and finite thickness effects also in the linear viscoelastic case. The proposed periodic formulation is particularly helpful in this paper where, in order to investigate the role of finite thickness, contact solutions with large contact areas need to be treated: the periodic formulation enables us to eliminate any border effects, hence eliminating any spurious contribution that finite size domains may cause.

3. Results and discussion

Results shown in next subsections are referred to the contact between a deformable - elastic or viscoelastic- layer and rigid fractal self-affine surface numerically generated by means of the spectral method described in [33]. These surfaces have spectral components in the range $q_0 < q < q_1$, where $q_0 = 2\pi/L$ with L the size of the square computational cell and $q_1 = Nq_0$ being N the number of scales (or wavelengths). The surface employed in this paper is generated with $L = 0.01$ m, $N = 64$ and the Hurst coefficient $H = 0.75$. Results are obtaining averaging 10 different realizations of this surface.

3.1. Elastic materials

We study the contact between the rigid surface described above and an elastic layer with a Young modulus $E_0 = 7.5$ MPa and a Poisson's ratio $\nu = 0.5$. Results are shown for four different values of the dimensionless thickness h/L and, in particular, for $h/L \to +\infty$, $h/L = 0.1$, $h/L = 0.08$ and $h/L = 0.06$. In Figure 3, we show the relation between the dimensionless contact area A/A_0 and the dimensionless load σ_0/E^* being σ_0 the normal mean pressure $\sigma_0 = P/A_0$ and E^* the composite Young's modulus $E^* = E/(1-\nu^2)$. Indeed, no influence of the thickness is observed for very low loads; however, as soon as the load and, consequently, the contact areas increase, a large difference between the elastic half-space and the layers with finite thickness is found. In particular, the more the thickness decreases, the more the contact stiffness increases and, consequently, the smaller the areas are obtained for fixed load. This is perfectly consistent with the cut-off effect produced by the corrective coefficient Θ and described in Section II. Incidentally, we observe that, when the half-space assumption has put aside, the classical expression relating loads and real contact areas $A/A_0 = \kappa\sigma_0/E^*\sqrt{2m_2}$ with k approximately equal to $k = 2$ [33],[34] keeps its validity only for very low loads, i.e. when the contact clusters are really small. Indeed, for $h \to 0$, we have actually contact between two rigid bodies and $\kappa \to 0$. This has to be carefully considered when a simulation, like Finite Element Methodologies (FEM) [62] or Molecular Dynamics (MD) [61], needs to account also for the bulk region of the bodies in contact: insuffi-

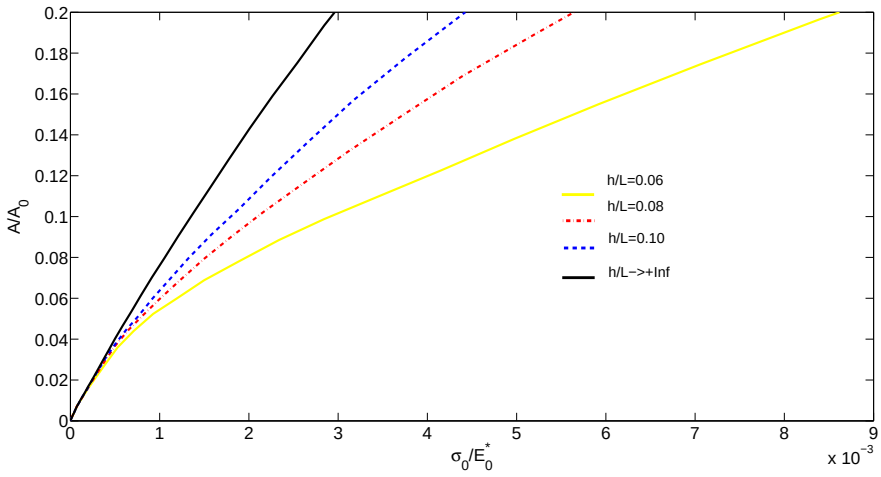

Figure 3: Contact area A/A_0 as a function of the dimensionless load σ_0/E^* for different values of the thickness h/L : $h/L- > +\infty$ (black curve), $h/L = 0.1$ (blue dotted curve), $h/L = 0.08$ (red dotted curve) and $h/L = 0.06$ (yellow curve).

ciently large thickness values can lead to a significant underestimation of the contact area .

Figure 4 shows the dimensionless separation s/h_{rms} as a function of the load σ_0/E^*. We observe that , at relatively high loads, in agreement with many theoretical and numerical predictions ([5],[34] , [30]), a logarithmic dependence between s/h_{rms} and σ_0/E^* is found. At smaller loads, such a behavior is lost due the finiteness of the rigid surface employed in the computations: indeed, when the separation overcomes the maximum value of the heights $h_{\max}$, no contact can occur and, therefore, for low loads, the logarithmic trend cannot keep on being valid. Interestingly, when changing the thickness of the deformable layer, such a trend is still present, but we find prominent quantitative changes: when the thickness is lowered, the contact

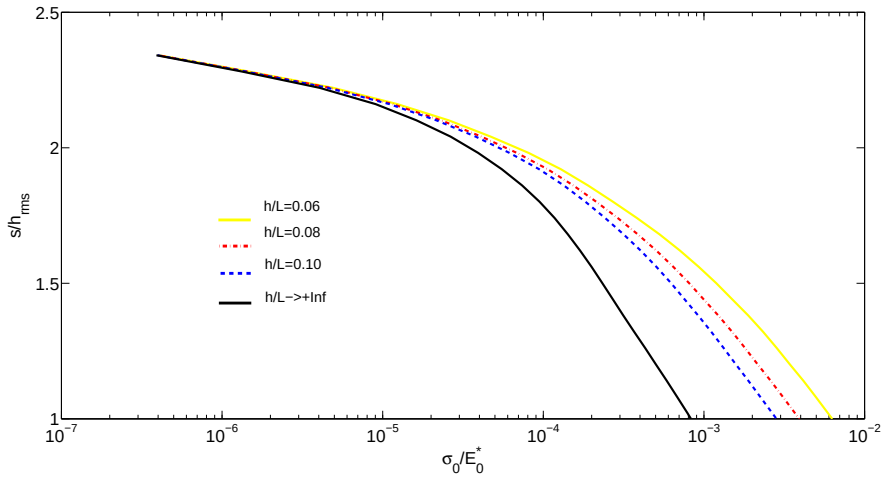

Figure 4: Dimensionless separation s/h_{rms} as a function of the dimensionless load σ_0/E^* for different values of the thickness h/L : $h/L- > +\infty$ (black curve), $h/L = 0.1$ (blue dotted curve), $h/L = 0.08$ (red dotted curve) and $h/L = 0.06$ (yellow curve).

stiffness grows and, fixed the load, the separation increases.

3.2. Viscoelastic materials

Let us now consider the case of the sliding contact between the same rigid surface and a viscoelastic layer with $E_\infty = 10^7$Pa, $E_\infty/E_0 = 3$, and $\tau = 0.01$s . Also in the case of viscoelastic materials, decreasing the thickness corresponds to increase the contact stiffness. This can be observed in Figure 5, where, fixed the load $\sigma_0/E^* = 4 \cdot 10^{-3}$, the contact area A/A_0 is shown as a function of the dimensionless sliding speed $\xi = v\tau/L$: fixed the speed, when the thickness decreases, we find smaller contact areas.

In Figure 6, we focus on the viscoelastic friction coefficient: as expected, for smaller thickness values and same values of speed, ξ, a smaller volume

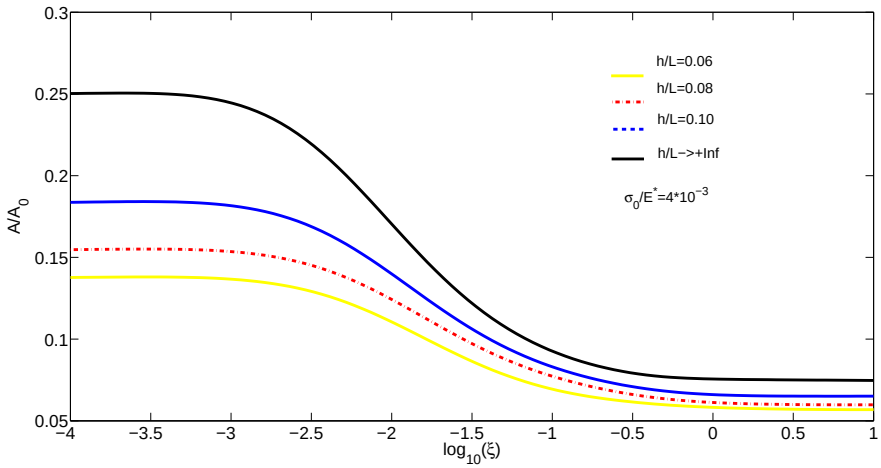

Figure 5: Contact area A/A_0 as a function of the dimensionless sliding speed $\xi = v\tau/L$ for the constant normal load $\sigma_0/E^* = 4 \cdot 10^{-3}$ and different values of the thickness h/L : $h/L- > +\infty$ (black curve), $h/L = 0.1$ (blue dotted curve), $h/L = 0.08$ (red dotted curve) and $h/L = 0.06$ (yellow curve).

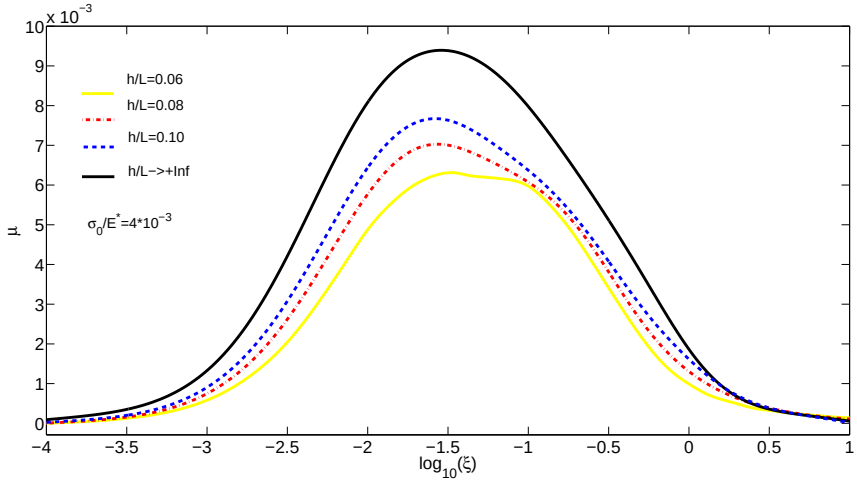

Figure 6: Vicoelastic friction coefficient μ as a function of the dimensionless sliding speed $\xi = v\tau/L$ for the constant normal load $\sigma_0/E^* = 4 \cdot 10^{-3}$ and different values of the thickness h/L : $h/L- > +\infty$ (black curve), $h/L = 0.1$ (blue dotted curve), $h/L = 0.08$ (red dotted curve) and $h/L = 0.06$ (yellow curve).

of material is deformed due to contact stiffening, and, therefore, the friction coefficient is lower. Furthermore, also the anisotropy of the contact solution decreases with the thickness, thus confirming the affinity between friction and contact anisotropy suggested by the authors in [52]. In Figure 7, we plot in a polar diagram $m_2(\theta)$ that is the average square slope of the a profile obtained by cutting the deformed surface $u(\mathbf{x};\zeta_1,\zeta_2)$ along the direction θ [51], for different values of the thickness. To quantify the anisotropy of the deformed surface, one can focus on the ratio $\gamma = m_{2\,\min}/m_{2\,\max}$ between the minimum $m_{2\,\min}$ and the maximum $m_{2\,\max}$ values of $m_2(\theta)$: when γ is equal to 1 and, so, the polar plot is a circumference, the deformed surface is perfectly isotropic; on the contrary, when γ is smaller than 1 and, therefore, we have an ellipse, the contact solution is anisotropic. In Figure 7, in all the four cases, we have an anisotropic solution, but the degree of anisotropy decreases with the thickness. Interestingly, the value of the angle θ_P which maximize $m_2(\theta)$, i.e. $m_2(\theta_P) = m_{2\,\max}$ is always close to 90° , thus confirming that, also for thin layers, the contact area results stretched perpendicularly to the sliding speed.

However, the contact stiffening is not the only effect related to the finite layer thickness. This is somehow confirmed looking at Figure 6 , where the curves referred to $h/L = 0.1$, $h/L = 0.08$ and $h/L = 0.06$ do not have the classical bell shape marking the half-space case and, actually, show almost a plateau before decreasing for larger values of dimensionless speed. This trend is also clearly present and further accentuated in Figure 8, where, for

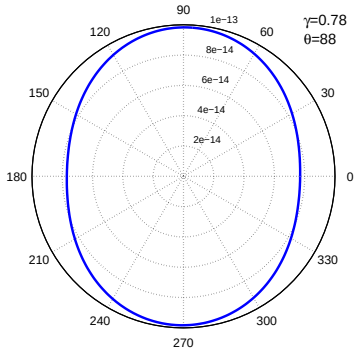

[a]

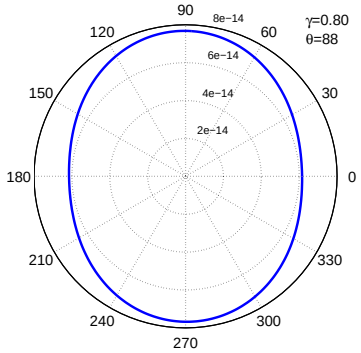

[b]

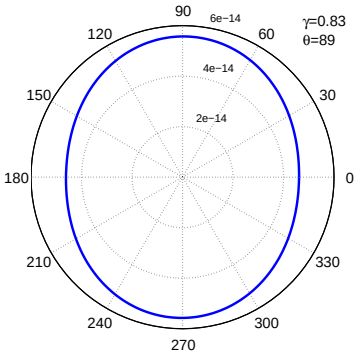

[c]

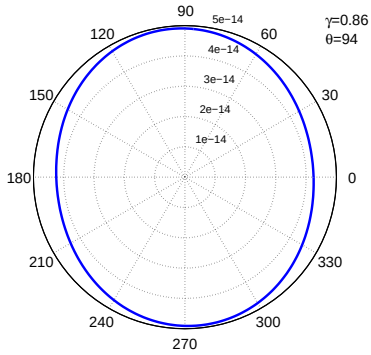

[d]

Figure 7: Polar plots of $m_2(\theta)$ for a dimensionless sliding speed value $\xi = 0.01$ and a constant normal load $\sigma_0/E^* = 4 \cdot 10^{-3}$. The four polar plots are referred to different values of the thickness h/L : $h/L- > +\infty$, $h/L = 0.1$, $h/L = 0.08$ and $h/L = 0.06$.

the thickness value $h/L = 0.06$ and for different normal load σ_0/E^*, the friction coefficient is shown as a function of the dimensionless speed. We observe that the friction coefficient curve has the usual bell-shaped behavior only for the lowest normal load $\sigma_0/E^* = 10^{-3}$, whereas for the highest value $\sigma_0/E^* = 10^{-2}$ a completely different trend, with two maximum points, is observed. Furthermore, it is surprising to notice that the friction coefficient decreases with the normal load; one would expect to have more dissipation when the deformed volume increases due to viscoelastic losses. To explain such a behavior, we should focus on the physics governing viscoelastic friction: this is due to the dissipation happening in the material volume deformed during the sliding motion. Now, when the contact layer has a finite thickness, the amount of material, which can be deformed and, consequently, can dissipate, is finite: once the region available for the dissipation to take place is saturated, no further increase of the friction coefficient can be obtained by increasing the normal force. This is clarified in Figure 9, where a schematic shows that in the layered case the region capable of dissipating is saturated and the saturation depends on the relative sliding speed for the viscoelastic case.

In order to explore this behavior it is necessary to introduce a characteristic length, l_{eq}, which qualitatively captures the extent of the dissipative region; this allows a direct comparison with the other key length scale of the problem, namely the thickness, h, of the viscoelastic layer. This characteristic length should be ideally defined so that it can capture the saturation of the

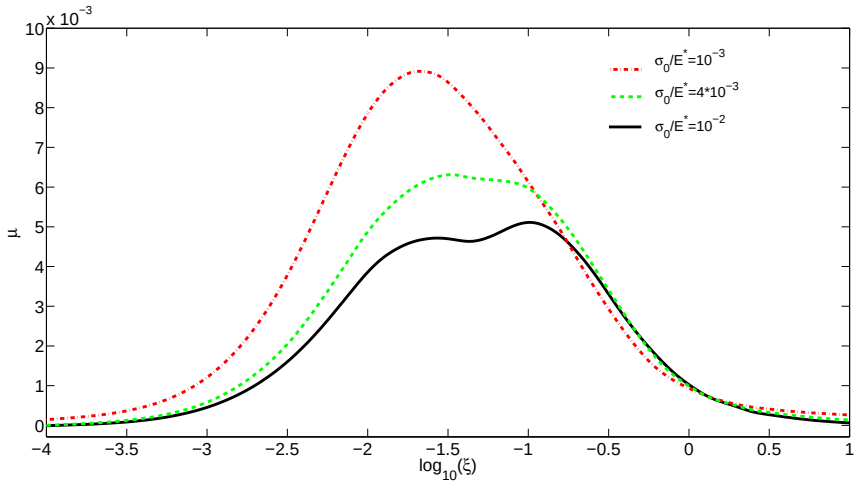

Figure 8: Vicoelastic friction coefficient μ as a function of the dimensionless sliding speed $\xi = v\tau/L$ for the constant thickness $h/L = 0.06$ and different values of the normal load σ_0/E^* : $\sigma_0/E^* = 10^{-2}$ (black curve), $\sigma_0/E^* = 4\,10^{-3}$ (green dotted curve), $\sigma_0/E^* = 10^{-2}$ (red dotted curve).

material's capability to dissipate. In particular, if l_{eq} is thought as a mono-dimensional measure of the volume over which dissipation takes place, when the ratio l_{eq}/h is smaller than 1 there is still material capable of dissipating; conversely, as soon as l_{eq}/h becomes greater than 1, the dissipative region gets saturated. In contact problems characterized by regular or smooth surfaces, it would be straightforward to define l_{eq} as the contact characteristic wavelength or contact width respectively; however, it is less easy to define a unique wavelength for a specific contact problem when dealing with multi-scale rough surfaces. In this paper, we choose to define l_{eq} as $l_{eq} = \sqrt{A_m}$, where A_m is the mean value of the individual clusters in the contact area. Despite this choice is somehow arbitrary, we underline that this definition

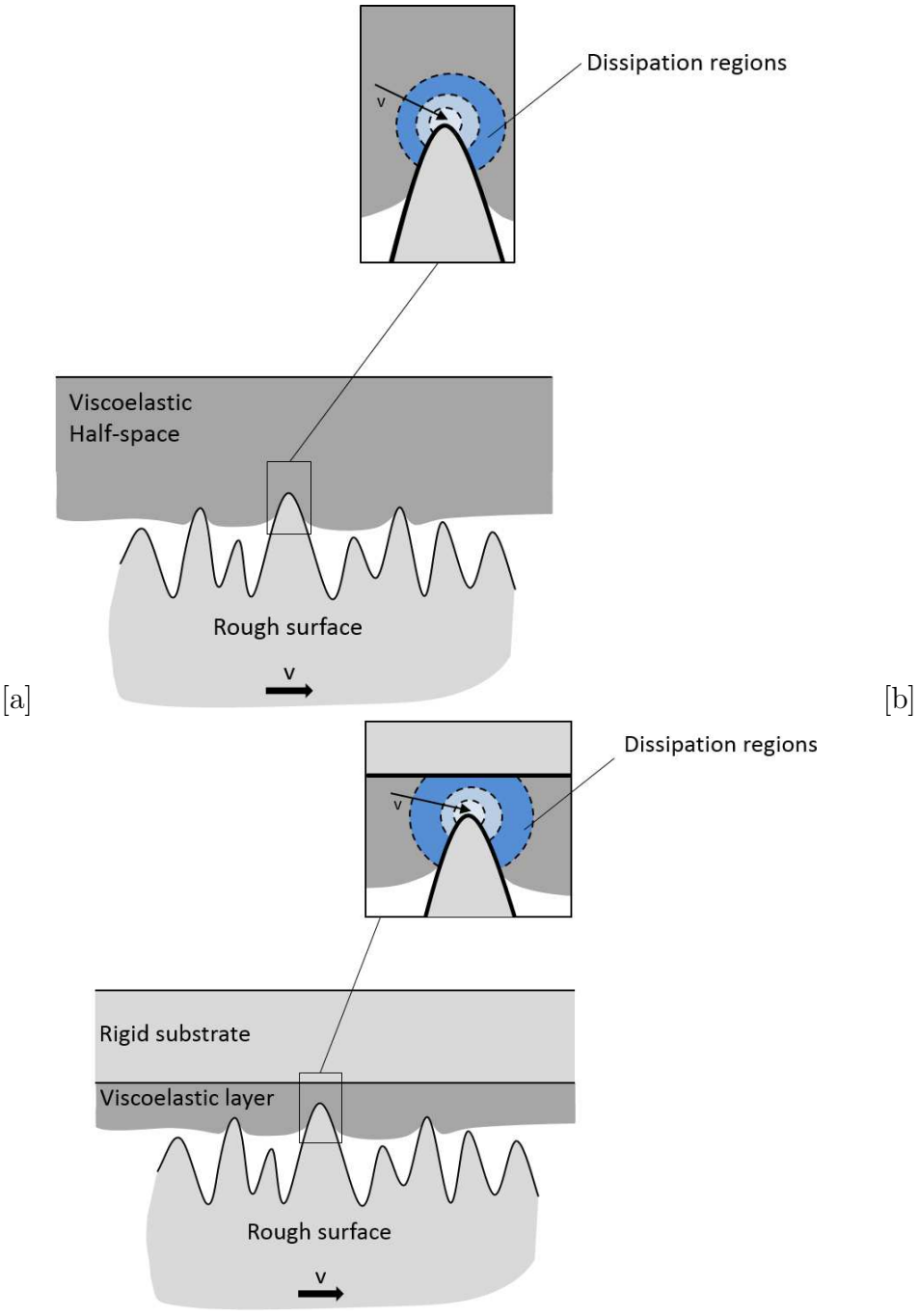

Figure 9: Schematic of the viscoelastic friction for half-space and for a thin layer .

would be rigorous in the case of a single scale rough surface in full contact conditions, where this choice would coincide with a uniquely defined contact characteristic wavelength. In Figure 10 , we plot the ratio l_{eq}/h as a function of the dimensionless speed ξ for the same load values studied in Fig. 8. Interestingly, we observe that l_{eq}/h is not constant but depends on the sliding speed, and two different regimes can be observed, especially in the case of the highest load value $\sigma_0/E^* = 10^{-2}$. Indeed, we can distinguish between speed ranges where the material is saturated ($l_{eq}/h > 1$) and intervals where the layer still has more material available for dissipating ($l_{eq}/h < 1$). It is noteworthy to observe how the plateau shown by the curve in Figure 8 and the the two maxima obtained in the friction response correspond to the transition between the two regions in Figure 10. It is clearly shown that when the ratio l_{eq}/h becomes smaller than 1 and, therefore, there is material that can be added to the region in which viscoelastic losses take place, instead of going on decreasing, the friction coefficient starts increasing again; this corresponds to the second maximum developing on the friction response plot in Fig. 8. We notice that, for the lowest load $\sigma_0/E^* = 10^{-3}$, no saturation is present and, consequently, the friction coefficients values are higher than the cases when saturation of the dissipative layer occurs.

The transition between two different regimes is observed also in Figure 11, where we plot the dimensionless separation s/h_{rms} as a function of the speed ξ . Interestingly, we observe that, when the material has reached saturation, the stiffness decreases and lower separation values are allowed.

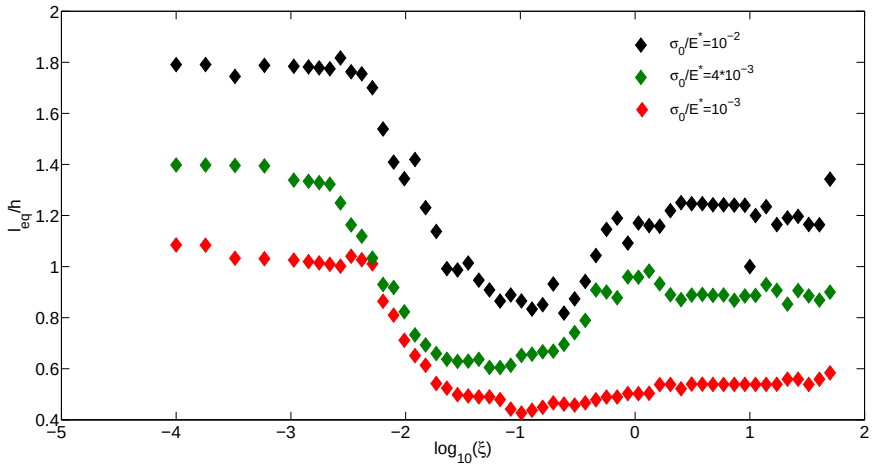

Figure 10: Ratio l_{eq}/h as a function of the speed ξ for the fixed thickness $h/L = 0.06$ and different levels of load: and different values of the normal load σ_0/E^* : $\sigma_0/E^* = 10^{-2}$ (black dots), $\sigma_0/E^* = 4\ 10^{-3}$ (green rhomboids), $\sigma_0/E^* = 10^{-2}$ (red dots).

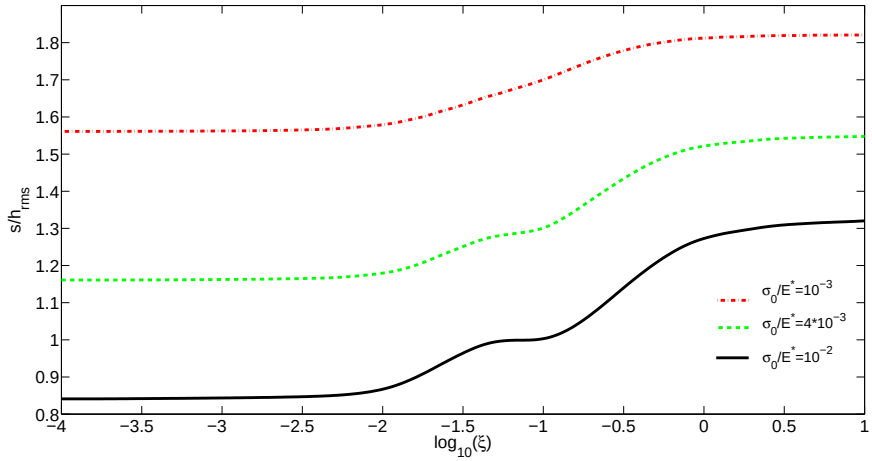

Figure 11: Dimensionless separation s/h_{rms} as a function of the dimensionless sliding speed $\xi = v\tau/L$ for the constant thickness $h/L = 0.06$ and different values of the normal load σ_0/E^* : $\sigma_0/E^* = 10^{-2}$ (black curve), $\sigma_0/E^* = 4\ 10^{-3}$ (green dotted curve), $\sigma_0/E^* = 10^{-2}$ (red dotted curve).

4. Conclusions

In this paper, we investigate the contact between rough bodies characterized by a finite thickness of layers of material bonded to a rigid substrate; the formulation presented by the authors overcomes the traditional half-space limitations. Accounting for the finite thickness of components subjected to contact is of crucial importance for a number of applications (in both industrial and biomechanical fields), e.g. when one of the contacting bodies is really thin or, similarly, is made of a thin coating attached to a stiffer substrate. In order to successfully develop a strategy to model this important class of contact problems, we have introduced a Boundary Element Method capable of accounting for the finite thickness of layers bonded to rigid substrates in a periodic domain by the means of the corrective coefficient Θ. This is used to modulate the Green's function, $\mathcal{T}(\mathbf{x})$, employed to solve the discretized problem and to obtain a finite correlation length, l_c, defined as the length at which the Green's function $\mathcal{T}(\mathbf{x})$ tends to 0 . This has as direct consequence the increase of the contact stiffness. The proposed periodic formulation provides for the first time the tools to explore a wide range of contact problems in the presence of layered bodies and enables us to overcome some of the limitations of the formulations proposed in Refs. [3] and [52]. Therefore, the newly developed algorithm has been used to perform a systematic investigation of a variety of contact problems characterised by layered elastic and viscoelastic materials subjected to various loads and sliding speeds. In the elastic case we observe that, by decreasing the dimensionless thickness, h/L

, and applying the same normal load σ_0/E^*, we obtain a smaller contact area and a higher separation. In other words, as expected observing the physics of the problem, decreasing the thickness means increasing the contact stiffness. When $h- > 0$ the stiffness tends to infinity since the problem degenerates towards the contact between two rigid bodies (indenter and substrate). In the viscoelastic case, this stiffening effect is still present, but the problem has to be analyzed more carefully. In particular, we observe that the viscoelastic friction is due to the dissipation occurring in the bulk of the material; however, unlike what happens for cases where the half-space configuration is studied, when dealing with layers of finite thickness the amount of material that can dissipate is finite and, once it is saturated, no further increase of the friction coefficient is possible. Since the dissipating region characteristic length is found to be in close relation to the mean value of the contact area clusters, we can have different behavior for the same layered system simply by changing the sliding speed; in particular, the transition between a saturated region and a regime still capable of increased dissipation has been identified. This can entail friction coefficient trends that cannot be explained without the fuller understanding of the physical mechanisms governing dissipation and material response provided by the investigation carried out in this paper; we have also shown that the results obtained using the newly developed technique can be very different from the results obtained in the half-space case [52].

5. References

[1] Geim, A.K., Dubonos, S.V., Gricorieva, I.V., Novoselov, K.S., Zhukov, A.A., Shapoval, S.Yu., Microfabricated adhesive mimicking gecko foot-hair. Nature Materials, 2, 461–463, (2003).

[2] Bhushan B., Springer Handbook of Nanotechnology, Springer, Berlin, Heidelberg, New York, (2004).

[3] G. Carbone, C. Putignano, A novel methodology to predict sliding/rolling friction in viscoelastic materials: theory and experiments. Journal of Mechanics and Physics of Solids, DOI: 10.1016/j.jmps.2013.03.005 .

[4] Hunter S.C. , The rolling contact of a rigid cylinder with a viscoelastic half space Trans. ASME, Ser. E, J. Appl. Mech. 28, 611–617 (1961).

[5] Persson B.N.J., Rolling friction for hard cylinder and sphere on viscoelastic solid, Eur. Phys. J. E **33**, 327-333 (2010).

[6] Panek C. and Kalker J.J., Three-dimensional Contact of a Rigid Roller Traversing a Viscoelastic Half Space, J. Inst. Maths Applies 26, 299-313, (1980).

[7] M. Harrass, K.Friedrich , A.A.Almajid,Tribological behavior of selected engineering polymers under rolling contact, Tribology International,43, 635–646, 2010.

[8] Grosch K. A. , The Relation between the Friction and Visco-Elastic Properties of Rubber, Proceedings of the Royal Society of London. Series A, Mathematical and Physical,274-1356, pp. 21-39, (1963).

[9] Carbone G., Lorenz B., Persson B.N.J. and Wohlers A., Contact mechanics and rubber friction for randomly rough surfaces with anisotropic statistical properties, The European Physiscal Journal E – Soft Matter, **29** (3), 275–284, (2009)

[10] Carbone G., Mangialardi L., Adhesion and friction of an elastic half-space in contact with a slightly wavy rigid surface, Journal of the Mechanics and Physics of Solids, **52** (6), 1267-1287, 2004.

[11] Putignano, C., Reddyhoff, T., Carbone, G., Dini, D., Experimental investigation of viscoelastic rolling contacts: A comparison with theory. Tribology Letters 51 (1) , pp. 105-113, 2013.

[12] Persson B.N.J.,Theory of rubber friction and contact mechanics, Journal of Chemical Physics,**115**, 3840 -3861(2001).

[13] Mandelbrot B. B., The Fractal geometry of nature, New York: W. H. Freeman and company, (1982).

[14] B.N.J. Persson, Contact mechanics for randomly rough surfaces, Surface Science Reports 61 201-227,(2006).

[15] Lorenz B.; Persson B. N. J.; Dieluweit S., tada T., Rubber friction: Com-

parison of theory with experiment, EUROPEAN PHYSICAL JOURNAL E **34** (12), 129, doi: 10.1140/epje/i2011-11129-1 (2011).

[16] Bottiglione F., Carbone G., Mangialardi L., Mantriota G., Leakage Mechanism in Flat Seals, Journal of Applied Physics 106 (10), 104902, (2009).

[17] Martina D.; Creton C.; Damman P.; et al., Adhesion of soft viscoelastic adhesives on periodic rough surfaces, Soft Matter **8** (19), 5350-5357, doi: 10.1039/c2sm07059f (2012)

[18] Carbone G., Pierro E., Gorb S., Origin of the superior adhesive performance of mushroom shaped microstructured surfaces, Soft Matter 7 (12), 5545-5552, DOI:10.1039/C0SM01482F, (2011).

[19] Carbone G., Pierro E., Sticky bio-inspired micropillars: Finding the best shape, SMALL, 8 (9), 1449-1454, doi: 10.1002/smll.201102021 (2012)

[20] Carbone G., Pierro E., Effect of interfacial air entrapment on the adhesion of bio-inspired mushroom-shaped micro-pillars, **8** (30), 7904-7908, doi:10.1039/C2SM25715G, (2012).

[21] Le Tallec P., Rahler C., Numerical models of steady rolling for non-linear viscoelastic structures in finite deformations,International Journal for Numerical Methods in Engineering, vol. 37, 1159-1186 (1994).

[22] Vollebregt E.A.H., User guide for CONTACT, J.J. Kalker's variational contact model, Technical Report TR09-03, version 1.18

[23] L. Afferrante, G. Carbone, G. Demelio & N. Pugno. Adhesion of Elastic Thin Films: Double Peeling of Tapes Versus Axisymmetric Peeling of Membranes. Tribol Lett DOI 10.1007/s11249-013-0227-6

[24] J. Padovan, O. Paramadilok, Transient and steady state viscoelastic rolling contact, Comput Struct, 20, 545-553, 1984.

[25] Nackenhorst U, The ALE-formulation of bodies in rolling contact Theoretical foundations andfinite element approach, Comput Method Appl M, 193, 4299-4322, 2004.

[26] Christensen R. M., Theory of viscoelasticity,Academic Press, New York.

[27] Carbone G., Scaraggi M., Tartaglino U., Adhesive contact of rough surfaces: comparison between numerical calculations and analytical theories", The European Physiscal Journal E – Soft Matter, **30** (1), 65–74 (2009).

[28] Putignano C., Afferrante L., Mangialardi L., Carbone G., Equilibrium states and stability of pre-tensioned adhesive tapes Beilstein J. Nanotechnol. 2014, 5, 1725-1731, doi:10.3762/bjnano.5.182.

[29] Carbone G., Pierro E., The influence of the fractal dimension of rough profiles on the adhesive contact of elastic materials, Journal of Adhesion Science and Technology, **26** (22), 2555-2570, DOI:10.1163/156856111X623140 (2012).

[30] Campana C.; Persson B. N. J.; Mueser M. H., Transverse and normal interfacial stiffness of solids with randomly rough surfaces, Journal of Physics-Condensed Matter **23** (8), 085001, doi: 10.1088/0953-8984/23/8/085001 (2011)

[31] Campana C.; Mueser M. H.; Robbins M. O., Elastic contact between self-affine surfaces: comparison of numerical stress and contact correlation functions with analytic predictions, Journal of Physics-Condensed Matter **20** (35) 354013, doi: 10.1088/0953-8984/20/35/354013 (2008).

[32] Carbone G. , Bottiglione F., Asperity contact theories: Do they predict linearity between contact area and load?, Journal of the Mechanics and Physics of Solids, 56, 2555-2572, (2008).

[33] Putignano C., Afferrante L., Carbone G., Demelio G. A new efficient numerical method for contact mechanics of rough surfaces. International Journal of Solids and Structures, 49 (2), 338-343, DOI 10.1016/j.ijsolstr.2011.10.009, (2012).

[34] Putignano C. , Afferrante L. , Carbone G. , . Demelio G, The influence of the statistical properties of self-affine surfaces in elastic contact: a numerical investigation, Journal of the Mechanics and Physics of Solids 60 (5), 973-982, Journal of Mechanics and Physics of Solids, (2012).

[35] Dapp W B, Prodanov N,and Müser M H , Systematic analysis of Pers-

son's contact mechanics theory of randomly rough elastic surfaces. J. Phys.: Condens. Matter 26 355002, (2014).

[36] Carbone G., Mangialardi L.: Analysis of adhesive contact of confined layers by using a Green's function approach, The Journal of the Mechanics and Physics of Solids, **56** (2), 684-706 (2008)

[37] D. Felhõs, D. Xu1, A. K. Schlarb, K. Váradi, T. Goda, Viscoelastic characterization of an EPDM rubber and finite element simulation of its dry rolling friction, eXPRESS Polymer Letters 2, 3,157–164, 2008 .

[38] Johnson K.L.J., Contact Mechanics, Cambridge University Press (1985).

[39] Longuet-Higgins M.S., The statistical analysis of a random, moving surface, Philosophical Transactions of the Royal Society of London. Series A, Mathematical and Physical Sciences, **249** (966), 321-387 (1957)

[40] Scaraggi M., Carbone G., Persson B.N.J., Dini D., Lubrication in soft rough contacts: A novel homogenized approach. Part I – Theory, Soft Matter 7 (21), 10395-10406, DOI:10.1039/C1SM05128H, (2011).

[41] J. A. Greenwood and J. B. P. Williamson, Contact of Nominally Flat Surfaces, Proc. R. Soc. Lond. A, 295 (1442), 300-319 (1966)

[42] Greenwood J.A.,A simplified elliptic model of rough surface contact, Wear 261 191–200 (2006).

[43] Greenwood, J.A., Putignano, C., Ciavarella, M. A Greenwood & Williamson theory for line contact. Wear. 270, 332-334, (2011).

[44] Bush A.W. ,Gibson R.D. ,Thomas T.R. , The elastic contact of a rough surface, Wear 35 87–111 (1975).

[45] Ciavarella M., Delfine V., Demelio G., A "re-vitalized" Greenwood and Williamson model of elastic contat between fractal surfaces, Journal of the Mechanics and Physics of Solids, 54, 2569–2591, (2006).

[46] Carbone G. , Bottiglione F., Asperity contact theories: Do they predict linearity between contact area and load?, Journal of the Mechanics and Physics of Solids 56 2555– 2572 (2008).

[47] Geike T.,Popov V. L., Mapping of three-dimensional contact problems into one dimension, Physical Review E, 76, 036710,(2007).

[48] Putignano, C., Afferrante, L., Carbone, G., Demelio, G.P., A multiscale analysis of elastic contacts and percolation threshold for numerically generated and real rough surfaces, Tribology International 64 , pp. 148-154, 2013.

[49] Scaraggi, M., Putignano, C., Carbone, G., Elastic contact of rough surfaces: A simple criterion to make 2D isotropic roughness equivalent to 1D one, Wear 297 (1-2) , pp. 811-817, 2013.

[50] M.L. Williams, R.F. Landel, J.D. Ferry, J. Amer. Chem. Soc., 77:3701, 1955.

[51] J. I. McCool, Characterization of surface anisotropy, Wear, 49 (1978), pp. 19–31.

[52] G. Carbone, C. Putignano. Rough viscoelastic sliding contact: theory and experiments. Physical Review E, 89, 032408, (2014).

[53] M Ciavarella, JA Greenwood, M Paggi. Inclusion of "interaction" in the Greenwood and Williamson contact theory. Wear, 265, 729–734, (2008).

[54] Paggi M. and Ciavarella M.. The coefficient of proportionality between real contact area and load, with new asperity models. Wear, 268, 1020-1029, (2010).

[55] V. A. Yastrebov, G. Anciaux, and J. F. Molinari, Contact between representative rough surfaces. Phys. Rev. E 86, 035601(R), 2012.

[56] Hyun S. ,Pei L. , MolinariJ.-F. and Robbins M. O.,Finite-element analysis of contact between elastic self-affine surfaces, Physical Review E, 70, 026117 (2004).

[57] A. Sackfield, D A Hills , D. Nowell. Mechanics of Elastic Contacts. Butterworth-Heinemann, 1993.

[58] Dini D, Nowell D, 2004, Flat and rounded fretting contact problems in-

corporating elastic layers, International Journal of Mechanical Sciences, 46, 1635-1657.

[59] Limbert, Georges and Middleton, John A transversely isotropic visco-hyperelastic material: application to the modelling of biological soft connective tissues. International Journal of Solids and Structures, 41, (15), 4237-4260, (2004).

[60] C. Flynn, A. Taberner, P. Nielsen. Modeling the Mechanical Response of In Vivo Human Skin Under a Rich Set of Deformations.Annals of Biomedical Engineering. 39, 7, 1935-1946, 2011.

[61] Yang C., Persson B.N.J., Molecular Dynamics Study of Contact Mechanics: Contact Area and Interfacial Separation from Small to Full Contact,Physical Review Letters, 100, 024303,(2008).

[62] Yang C., Tartaglino U., Persson B.N.J., A multiscale molecular dynamics approach to contact mechanics, Eur. Phys. J. E Soft-Matter, 19, 1 , 47–58, (2006).

[63] Campana, C, Muser, M.H., Contact mechanics of real vs. randomly rough surfaces: A Green's function moleculardynamics study, Europhysics Letters, 77, 3, 38005, (2007).

[64] Hyun S.and Robbins M. O., Elastic contact between rough surfaces: Effect of roughness at large and small wavelengths,Tribology International, 40 , 413–1422,(2007).

[65] Luan B. Q.,Hyun S. , Molinari J. F.,Bernstein N. and Robbins M. O.,Multiscale modeling of two-dimensional contacts, Physical Review E 74, 046710, (2006).

[66] Campañá C. , Müser M. H., Practical Green's function approach to the simulation of elastic semi-infinite solids, Phys. Rev. B 74, 075420, (2006).

[67] Benassi A., Vanossi A ., Santoro GE , Tosatti E., Optimal energy dissipation in sliding friction simulations, Tribology Letters 48 (1), 41-49, (2012).

[68] Pastewka L, Sharp TA, Robbins MO Seamless elastic boundaries for atomistic calculations. Phys Rev B 86(7):075459, (2012).